JOURNAL OF VIROLOGY, Dec. 2007, p. 13681–13693 Vol. 81, No. 24
0022-538X/07/$08.00+0 doi:10.1128/JVI.01702-07

Altered Pathogenesis of Porcine Respiratory Coronavirus in Pigs due to Immunosuppressive Effects of Dexamethasone: Implications for Corticosteroid Use in Treatment of Severe Acute Respiratory Syndrome Coronavirus[▽]

Kwonil Jung, Konstantin P. Alekseev, Xinsheng Zhang, Doo-Sung Cheon, Anastasia N. Vlasova, and Linda J. Saif*

Food Animal Health Research Program, Ohio Agricultural Research and Development Center, The Ohio State University, Wooster, Ohio 44691

Received 6 August 2007/Accepted 28 September 2007

The pathogenesis and optimal treatments for severe acute respiratory syndrome (SARS) are unclear, although corticosteroids were used to reduce lung and systemic inflammation. Because the pulmonary pathology of porcine respiratory coronavirus (PRCV) in pigs resembles SARS, we used PRCV as a model to clarify the effects of the corticosteroid dexamethasone (DEX) on coronavirus (CoV)-induced pneumonia. Conventional weaned pigs ($n = 130$) in one of four groups (PRCV/phosphate-buffered saline [PBS] [$n = 41$], PRCV/DEX [$n = 41$], mock/PBS [$n = 23$], and mock/DEX [$n = 25$]) were inoculated intranasally and intratracheally with the ISU-1 strain of PRCV (1×10^7 PFU) or cell culture medium. DEX was administered (once daily, 2 mg/kg of body weight/day, intramuscularly) from postinoculation day (PID) 1 to 6. In PRCV/DEX pigs, significantly milder pneumonia, fewer PRCV-positive cells, and lower viral RNA titers were present in lungs early at PID 2; however, at PID 4, 10, and 21, severe bronchointerstitial pneumonia, significantly higher numbers of PRCV-positive cells, and higher viral RNA titers were observed compared to results for PRCV/PBS pigs. Significantly lower numbers of $CD2^+$, $CD3^+$, $CD4^+$, and $CD8^+$ T cells were also observed in lungs of PRCV/DEX pigs than in those of PRCV/PBS pigs at PID 8 and 10, coincident with fewer gamma interferon (IFN-γ)-secreting cells in the tracheobronchial lymph nodes as determined by enzyme-linked immunospot assay. Our results confirm that DEX treatment alleviates PRCV pneumonia early (PID 2) in the infection but continued use through PID 6 exacerbates later stages of infection (PID 4, 10, and 21), possibly by decreasing cellular immune responses in the lungs (IFN-γ-secreting T cells), thereby creating an environment for more-extensive viral replication. These data have potential implications for corticosteroid use with SARS-CoV patients and suggest a precaution against prolonged use based on their unproven efficacy in humans, including possible detrimental secondary effects.

Severe acute respiratory syndrome (SARS) is a recent emergent zoonotic disease of humans caused by a new strain of coronavirus (CoV), likely originating from wild or captive bats within the region of the original SARS outbreak (25, 30, 32, 41). The global SARS epidemic began in Guangdong Province, Southern China, in November 2002 and within 6 months rapidly spread to more than 30 countries through the international travel of SARS carriers. The global epidemic was contained after more than 8,422 cases and 916 deaths, with a case fatality rate of 11% (61). Although civet cats and raccoon dogs have been considered as a natural reservoir for the SARS epidemic (2002-2003) (16, 39), these animals may have served only as an amplification host for SARS-associated CoV (SARS-CoV) to permit efficient animal-to-human and human-to-human transmission as determined by further genetic analysis (30, 59). Since termination of the epidemic in July 2003, new cases of SARS have emerged sporadically in East Asia, including the original site in Southern China (42). Most of the cases have been associated with laboratory-acquired virus exposure or zoonotic (animal-to-human) sporadic transmission. However, the potential for future outbreaks of human SARS-CoV and animal (zoonotic) SARS-CoV-associated disease in humans remains, because CoVs are known to evolve altered cellular tropism and host specificity (42).

SARS-CoV belongs to subgroup 2b of the group 2 CoVs (group 2a: human CoV OC43, murine hepatitis virus, bovine CoV, and porcine hemagglutinating encephalitis virus) in the family *Coronaviridae*, order *Nidovirales*, based on rooted-tree phylogenetic analysis (48). SARS-CoV causes severe lower respiratory tract disease in humans (5, 8, 11, 13, 22, 34, 35, 39, 51). The infection is characterized by acute damage of alveolar and bronchiolar epithelial cells, especially type 2 pneumocytes, in the acute phase of pneumonia, proliferative and fibrinous pneumonia, and pulmonary tissue damage due to immunopathology caused by activated inflammatory leukocytes and leukocyte-derived cytokines within the pulmonary lesions and in the blood of SARS patients at either early or late stages of the disease (5, 8, 11, 13, 22, 34, 35, 51). Such a pronounced immune response, including up-regulation of proinflammatory cytokines and chemokines, exacerbates the atypical pneumonia

* Corresponding author. Mailing address: Food Animal Health Research Program, Ohio Agricultural Research and Development Center, The Ohio State University, 1680 Madison Ave., Wooster, Ohio 44691. Phone: (330) 263-3744. Fax: (330) 263-3677. E-mail: saif.2@osu.edu.

▽ Published ahead of print on 17 October 2007.

and is characterized by a dry cough, persistent fever, and progressive dyspnea in SARS patients (5).

During the 2002-2003 SARS season, most clinicians used corticosteroids to modify the SARS symptoms based on anecdotal experience and on an incomplete understanding of tissue damage caused by the hyperimmune response in patients (14). At the time, the use of corticosteroids was thought to modify the hyperimmune response and to alleviate the SARS pneumonic lesions which led to acute respiratory distress syndrome (14, 20, 29, 49). Currently, however, many researchers have reported that the use of corticosteroids in SARS patients caused significant adverse effects, including fatal secondary viral/fungal/bacterial infections due to the immunosuppressive effects, steroid-induced avascular necrosis and myopathy, and ultimately an increased risk of either mortality or intensive care support requiring mechanical ventilation (1, 7, 13, 15, 18, 21, 22, 31, 36, 56). Corticosteroid therapy for SARS patients remains controversial, and there is no appropriate animal model that adequately reproduces the progression of the disease and the severe atypical pneumonia (15, 27). Once animal studies define the effects of corticosteroids on SARS-CoV-induced pneumonia or animal respiratory CoV-induced pneumonia, clinical management in humans can be designed more effectively to determine the best therapeutic approach with appropriate dosages, timing, and duration of corticosteroid treatment for SARS patients.

Porcine respiratory coronavirus (PRCV), a spike (S) gene deletion mutant of transmissible gastroenteritis virus (TGEV), which causes acute epidemic diarrhea in neonatal piglets, is classified as a group 1 CoV (42, 44). Although most PRCV infections are mild or subclinical in pigs unless accompanied by dual or secondary infections, pulmonary lesions consisting of atypical pneumonia resembling that in SARS patients are almost invariably present (42, 44). The PRCV is a unique CoV among 15 animal and human CoVs of the 3 groups in causing pronounced lower respiratory tract disease like SARS (9, 17, 37, 42, 44). As with SARS, PRCV infection of young pigs is associated with transient viremia, often with extremely high titers of PRCV in lungs ($10^{8.3}$ median tissue culture infectious doses [$TCID_{50}$] per gram of lung tissue) and with extensive lung consolidation (60%) (9, 17). However, the lesions and severity observed varied according to the strain of PRCV (17, 23). The pulmonary pathogenesis of PRCV in pigs resembles that of SARS in many aspects (8, 9, 11, 13, 17, 22, 23, 34, 35, 37, 42, 44, 51). First, in the early phase of pneumonia (within 10 days after onset of flu-like symptoms in SARS), SARS-CoV and PRCV replicate primarily in bronchiolar and alveolar epithelial cells, especially type 2 pneumocytes, and induce cell damage. Secondly, SARS-CoV and PRCV have common histological characteristics, detected as interstitial pneumonia with type 2 pneumocyte hypertrophy and hyperplasia and inflammatory leukocyte infiltration in the late phase of pneumonia (10 days beyond symptom onset in SARS). Third, SARS-CoV and PRCV both induce pneumonia with two phases, an early inflammatory phase and a late proliferative phase (approximately 10 days after symptom onset in SARS). This is distinct from most respiratory virus-induced pneumonias, in which only one of three possible phases (an inflammatory phase, a proliferative phase, or a fibrotic phase) occurs. Lastly, SARS-CoV and PRCV are detectable for long periods in the lung (up to day 42 for SARS and day 21 for PRCV in this study) compared to other acute human respiratory viruses (34). These data indicate that although the onset of symptoms in SARS-CoV patients is acute and sudden in most clinical cases, the pneumonia is induced later, often when symptoms and virus shedding appear to be resolving (11, 13, 22, 35, 51).

There are other differences and similarities between PRCV infection in pigs and SARS disease in humans. Unlike the case with SARS, there is less systemic proinflammatory cytokine activation found in pigs with PRCV infection, consistent with the usually mild clinical signs (55). Although extrapulmonary lesions are rare, PRCV was occasionally detected in the lamina propria of the small intestines of young infected pigs but without inducing intestinal villous atrophy, and it was present at low titers in the liver. The PRCV was also isolated at low titers from lymph nodes (bronchial, mesenteric, maxillary and parotid) and the spleen, but with lymphadenopathy observed (9, 17, 37, 42, 44). Similarly, the SARS-CoV-associated lesions or viral antigens/RNA have been identified in lymphoid organs (but with lymphocyte depletion), the liver, the gastrointestinal tract (with no significant pathological changes, as with PRCV), and feces, but in contrast to PRCV, also in the kidneys and urine (as tubular necrosis), central nervous system (as degeneration of neurons), and even bone marrow (as hemophagocytosis) of SARS patients (11, 34, 35, 51), most of whom received high-dose corticosteroids for a longer period than is the case after common viral infections (1, 3, 27).

The possibility remains that the use of corticosteroids in SARS patients contributed to the severity of SARS, including the risk of secondary viral/fungal/bacterial infections, rather than ameliorating the disease (1, 7, 13, 15, 18, 21, 22, 31, 36, 56). Therefore, studies to evaluate the impact of corticosteroid treatments and development of appropriate animal models for determining the influence of coinfections on the severity of SARS-CoV-induced respiratory diseases are needed. The goal of the current study was to clarify the effects of the corticosteroid dexamethasone (DEX), adopting a postinfection dosage regimen similar to that used for SARS patients, on PRCV pneumonia with a porcine disease model that mimics the atypical pneumonia and lesions seen in SARS patients.

MATERIALS AND METHODS

Animals and viruses. Large White-Duroc crossbred weaned pigs ($n = 130$) were obtained from sows that were serologically negative for porcine reproductive and respiratory syndrome virus (PRRSV), PRCV, and TGEV, from a specific-pathogen-free swine herd at the Ohio Agricultural Research and Development Center, Ohio State University, Wooster, OH. The swine herd also had no porcine circovirus type 2 (PCV2)-associated disease, i.e., postweaning multisystemic wasting syndrome and porcine respiratory disease complex in weaned pigs, porcine dermatitis and nephropathy syndrome in grower pigs, or PCV2-associated abortions or stillbirths in pregnant sows. The piglets were weaned at 20 days of age, allowed to acclimate for a week, and then transported to an isolation facility when 27 days old. After the 7-day acclimation to the isolation facility, corticosteroids and virus or mock-infected cell culture fluids were administered. The animals were given fresh water and pelleted feed. Each experimental group of pigs was housed in a separate room in a high-security isolation facility (biosafety level 2) in accordance with the guidelines of the Institutional Animal Care and Use Committee of Ohio State University. PRCV strain ISU-1, which originated from nasal swabs collected from infected pigs in Indiana (19), was plaque purified 2 times and passaged 14 times in swine testicle (ST) cells prior to use as an inoculum. For the inoculum, this strain was cultivated in ST cells in Eagle's minimal essential medium (MEM) (GIBCO/BRL) supplemented with antibiotic-

antimycotic solution (Gibco/BRL). Titers of virus were assayed by plaque assays as PFU (PFU/ml), as described previously (4).

Establishment of PRCV infection in pigs and DEX treatment. Pigs were randomly assigned to four groups: PRCV/PBS ($n = 41$), PRCV/DEX ($n = 41$), mock/PBS ($n = 23$), and mock/DEX ($n = 25$). A total of five independent experimental trials were performed between October 2005 and February 2007, as follows: trial 1, $n = 18$, in 2005; Trials 2 to 4, $n = 84$, in 2006; and Trial 5, $n = 28$, in 2007. Over the first 3 days of each experiment, prior to virus inoculation, a physical examination was performed to assess clinical signs and health of the animals (lethargy, sneezing, and coughing), body weight, respiratory rates, and rectal temperatures. For virus inoculation, the pigs were sedated by intramuscular injection of 6 mg tiletamine plus zolazepam (Telazol; Fort Dodge Animal Health, Fort Dodge, IA) per kg of body weight and 1 mg xylazine (Akom, Inc.) per kg of body weight. Pigs ($n = 82$) were then inoculated intranasally and intratracheally with 1×10^7 PFU of the PRCV strain ISU-1 or were inoculated with mock-infected cell culture medium ($n = 48$). DEX (Vedco, Inc.), an anti-inflammatory corticosteroid, was given daily to PRCV/DEX and mock/DEX pigs by intramuscular injection of 2 mg per kg of body weight from postinoculation day (PID) 1 to 6 to mimic the doses and regimen used for SARS patients (1, 14, 27). A previous report indicated that a single treatment of DEX (2 mg/kg) caused lymphopenia and a marked decrease in lymphocyte blastogenesis in pigs (12). The PRCV/PBS and mock/PBS pigs were similarly administered phosphate-buffered saline (PBS) (pH 7.4). After virus inoculation and DEX administration, pigs were assessed clinically every day and nasal swabs were collected every other day from each animal throughout the experiment (from PID 0 to PID 21). The swabs were placed in 4 ml of MEM supplemented with antibiotic-antimycotic solution and stored at −70°C until tested.

Evaluation of gross and histopathologic lesions. Four to nine pigs per group were euthanized, and specimens were collected at early (PID 2 and 4), middle (PID 8 and 10), and late (PID 21) stages of the infection. Euthanasia was performed by electrocution followed by exsanguination as recommended by the American Veterinary Medical Association panel report (2000). Complete necropsies were performed on all the pigs, and organs (lung, kidney, spleen, liver, tracheobronchial lymph nodes (TBLNs), jejunum, ileum, cecum, and colon) were examined grossly and histologically. For evaluation of macroscopic pulmonary lesions, the lungs were examined and were given an estimated score based on the percentage of virus-affected lesions (consolidation) in all six lobes (right cranial, middle and caudal, left cranial and caudal, and accessory lobes). The maximum gross lung lesion score was 10.875 if the lung was the most severely affected (100%). Sections of lung tissue were obtained from the left cranial lung lobe because PRCV-induced pneumonic lesions were characterized by cranioventral pneumonia, as identified in this study and in previous publications (9, 17, 22, 37). All tissue samples, which were sliced to no more than 1 cm in thickness, were rapidly fixed in freshly prepared 4% (wt/vol) paraformaldehyde in 0.1 M PBS (pH 7.4) overnight at 4°C. The tissues were dehydrated in a graded ethanol series and embedded in paraffin, and 3-μm sections were cut for histopathological examination, followed by hematoxylin-and-eosin staining. Tissue sections were evaluated blinded, without information on the infection status. Specifically, lung tissues were analyzed morphometrically and scored according to three parameters of pulmonary pathology: (i) thickening of alveolar septa by infiltration of inflammatory leukocytes, principally mononuclear cells, and type 2 pneumocyte hypertrophy and hyperplasia (ranging from 0 to 6, where 0 is normal appearance, 1 is mild focal or multifocal, 2 is mild diffuse, 3 is moderate focal or multifocal, 4 is moderately severe, 5 is severe focal or multifocal, and 6 is severe diffuse interstitial pneumonia); (ii) accumulation of necrotic cells and inflammatory leukocytes in alveolar and bronchiolar lumina due to airway epithelial necrosis (ranging from 0 to 3, where 0 is normal appearance and 3 is severe); and (iii) peribronchiolar or perivascular lymphohistiocytic inflammation (ranging from 0 to 3, where 0 is normal appearance and 3 is severe). The total histopathological lung lesion scores ranged from 0 (no abnormalities) to 12 (most severe bronchointerstitial pneumonia). In addition, to evaluate the degree of enlargement of the TBLNs following PRCV inoculation and any reduction following DEX treatment, the left TBLNs from each pig were weighed, and lymph-node-to-body-weight (LN/BW) ratios were calculated.

Immunohistochemistry (IHC) for detection and quantification of PRCV antigens. For detection of PRCV antigens in the tissues of PRCV-inoculated (PRCV/PBS and PRCV/DEX) and mock-inoculated (mock/PBS and mock/DEX) pigs, all tissue samples were prepared as described earlier. The tissue slides were incubated at 60°C for 20 min, deparaffinized in xylene twice for 5 min each, and rehydrated through a graded ethanol series (100% to 50%). Antigen retrieval was performed using 100 μg/ml of proteinase K (Invitrogen Corp.), and sections were immersed in 0.3% H_2O_2 in methanol to block endogenous peroxidase. The tissue slides were then washed in PBS three times and blocked with 1% normal goat serum for 30 min at room temperature. Three monoclonal antibodies (all diluted 1:200) against the nucleocapsid proteins (25H7 and 14E3) and the S protein (25C9) of TGEV, which cross-react with PRCV, were incubated with the tissues overnight at 4°C (46). The tissue sections were then washed twice in PBS and incubated with goat anti-mouse immunoglobulin G (IgG) labeled with horseradish peroxidase (1:200; Dako, CA) for 1 h at 37°C. Antibody binding was detected by immersing sections in a solution of 3,3′-diaminobenzidine substrate (BD Biosciences) for 10 min at room temperature. Sections were counterstained with Mayer's hematoxylin. PRCV antigen-positive scores were computed by estimating the number of PRCV-positive cells in the lung and other organ sections per microscopic area at magnification ×200 based on the following criteria: 0, no positive cells; 1, few (less than 10) positive cells; 2, moderate (from 11 to 25 positive cells), and 3, high (more than 26 positive cells).

Evaluation of virus shedding by CCIF, RT-PCR, and real-time PCR. To determine the extent and changes in patterns of virus shedding from nasal swabs, the nasal samples were tested using a cell culture immunofluorescence (CCIF) test, reverse transcription-PCR (RT-PCR), and real-time PCR. The CCIF test was performed as previously described (47). Briefly, fourfold serial dilutions of the nasal swab supernatants were inoculated onto ST cells grown in 96-well tissue culture plates and incubated for 18 h at 37°C in 5% CO_2. The cells were fixed with 80% acetone, stained with hyperimmune porcine anti-TGEV serum conjugated to fluorescein isothiocyanate, and analyzed by fluorescence microscopy. Titers were expressed as fluorescent focus units (FFU) per ml.

One-step RT-PCR was performed for the detection of PRCV RNA from nasal swabs, as described previously (24). Briefly, RNA was extracted from nasal swab samples using the TRIZOL LS reagent (Invitrogen) according to the manufacturer's instructions and precipitated with isopropanol to collect viral RNA. The RNA samples were diluted in diethyl pyrocarbonate-treated water. The forward and reverse primers used to detect PRCV were as follows: 5′-GGGTAAGTTG CTCATTAGAAATAATGG-3′ and 5′-CTTCTTCAAAGCTAGGGACTG-3′, respectively, which amplified the 325-to-385-bp region from open reading frame 1b and the S gene of PRCV. Viral RNA (5 ng) was used in a total reaction volume of 50 μl with 5 μl 10× PCR buffer (Promega, Madison, WI), 5 μl of 25 mM $MgCl_2$ (Promega, Madison, WI), 1 μl of 10 mM (each) deoxynucleoside triphosphates, 20 U RNasin (Promega, Madison, WI), 5 U avian myeloblastosis virus reverse transcriptase (Promega, Madison, WI), 2.5 U *Taq* DNA polymerase (Promega, Madison, WI), and 0.5 μl of each primer (50 pm stocks). The reference strains, PRCV strain ISU-1 and TGEV strain M6 Miller, were used as positive controls, and the negative controls included PRCV/TGEV-negative nasal swabs from mock-infected pigs and water. The PCR was carried out under the following conditions in a thermocycler (Applied-Biosystem): 90 min at 42°C, 5 min at 95°C, and then 35 cycles of denaturation at 94°C for 1 min, annealing at 60°C for 1 min, and extension at 72°C for 1 min, followed by a final cycle of extension at 72°C for 10 min. The PCR products were analyzed on 1.5% agarose gels stained with ethidium bromide. Real-time PCR was performed as described below.

Quantitative real-time PCR for PRCV RNA titers in lung and BAL fluids. For evaluation of PRCV RNA titers in lung tissues, bronchoalveolar lavage (BAL) fluids, and nasal samples of PRCV-infected and mock-infected pigs, a two-step real-time PCR was developed. Lung tissues were collected from each pig at necropsy and frozen rapidly at −70°C until use. The frozen lungs were cut, weighed, and placed in MEM for RNA extraction. To make homogenates, the tissues were blended for 2 min in a Stomacher 400 laboratory blender (Seward). BAL fluids were collected from either the right or left lung of each pig as previously described (26), with slight modifications. Briefly, the right lung was lavaged with 50 ml of MEM administered through the trachea. Approximately 50% of the initial volume of the lavage fluid was recovered. The BAL fluid was centrifuged at 800 × *g*, 4°C, for 10 min to separate cells, and the cell-free lavage fluids were stored at −70°C until use for RNA extraction. The BAL cells were used to determine the total number of cells and calculate the differential cell count, as previously described (26).

The PRCV RNA was extracted from lung tissue and BAL samples using the Qiagen RNeasy Mini kit (Qiagen, Inc.) according to the manufacturer's instructions. The primers for PRCV quantification were designed from nucleotide sequences of the nucleocapsid gene of TGEV (NCBI GenBank; accession number AF302264) using the primer select program in the DNAStar software (DNAStar, Inc.). A 244-bp region was amplified from the nucleocapsid gene of TGEV using forward (5′-GGCAACCCAGACAACTCCATC-3′, nucleotides 105 to 126) and reverse (5′-CTTCAACCCCATAACCCTCCAG-3′, nucleotides 328 to 348) primers. For first-strand cDNA synthesis, 2 μl of the PRCV RNA (5 ng/μl) was added to a total reaction volume of 20 μl with 1× RT buffer (50 mM Tris-HCl, 8 mM $MgCl_2$, 30 mM KCl, 1 mM dithiothreitol [pH 8.3]), 0.5 mM (each) deoxynucleoside triphosphates, 2.5 μM random hexanucleotide mixture

(Promega, Madison, WI), 20 U RNasin (Promega, Madison, WI), and 50 U avian myeloblastosis virus reverse transcriptase (Promega, Madison, WI). After incubation for 45 min at 42°C, the mixture was heated for 5 min at 99°C to denature the products and then stabilized at 4°C. The reference strains, PRCV strain ISU-1 and TGEV strain M6 Miller, were used as positive and negative controls along with PRCV/TGEV-negative nasal swabs from mock-infected pigs and water.

Real-time PCR was performed using the LightCycler DNA Master SYBR Green I kit (Roche Diagnostic, Mannheim, Germany). The cDNA (4 μl) was added to a total reaction volume of 25 μl with 2.5 μl 10× SYBR Green I mix, 1.25 μl 25 mM $MgCl_2$, and 0.5 μl of each primer (25 pmol stocks). The PCR was conducted under the following conditions in a SmartCycler real-time machine (Cepheid): 1 cycle of 2 min at 95°C and 40 cycles of denaturation at 95°C for 20 s, annealing at 60°C for 30 s, and extension at 72°C for 30 s. Melting-curve analysis was performed immediately after the amplification protocol under the following conditions: 0 s (hold time) at 95°C, 15 s at 65°C, and 0 s (hold time) at 95°C. Relative fluorescence units (RFU) for incorporated SYBR dyes were monitored during each cycle at 540 nm. The cycle threshold (C_T), which is the cycle number at which a positive amplification reaction was identified, was defined when the RFU exceeded 10 times the standard deviation of baseline RFU values of all samples. A standard curve was developed using 10-fold serial dilutions of the stock PRCV-ISU-1 strain (7.25×10^4 PFU/ml). The C_T values were plotted against virus quantity in $\log_{10}$ PFU/ml. The standard curve was used to convert C_T values for each specimen to PFU/ml equivalents. All samples were processed in duplicate. To determine the sensitivity of real-time PCR, a 10-fold dilution series of the tissue culture-grown PRCV-ISU-1 strain (7.25×10^4 PFU/ml) was made and nucleic acid was extracted for cDNA synthesis from each dilution. The real-time PCR test detected PRCV cDNA up to a dilution of 10^{-6}, corresponding to 0.0725 PFU/ml. In the specificity studies, PRRSV, PCV2, and swine influenza H1N1 virus were tested by real-time PCR, and there were no cross-reactions with these viruses.

Immunohistochemical detection of $CD2^+$, $CD3^+$, $CD4^+$, and $CD8^+$ T cells in lung tissue. Four commercially available mouse monoclonal antibodies (MAb) against porcine leukocyte antigens were used for detection of the $CD2^+$, $CD3^+$, $CD4^+$, and $CD8^+$ T-cell antigens in 4% paraformaldehyde-fixed, paraffin-embedded lung tissues of PRCV-infected and mock-infected pigs. IHC procedures were performed as previously described, with slight modifications (50). The MAb anti-CD4 (clone 74-12-4; Southern Biotechnology, Birmingham, AL), MAb anti-CD8 (clone 76-2–11; Southern Biotechnology), MAb anti-CD2 (VMRD, Inc., Pullman, WA), and MAb anti-CD3 (Southern Biotechnology) were all diluted 1:100 in PBTS (0.1% Tween 20 in 0.1 M PBS).

The paraffin-embedded lung tissues were sectioned at 3 μm thick and collected on positively charged slides (Fisher Scientific). Slides were kept at 60°C for 20 min, deparaffinized in xylene twice for 5 min each, and rehydrated through a graded ethanol series (100% to 50%). Antigen retrieval for $CD4^+$ and $CD8^+$ T-cell antigens was performed by digestion of tissue sections with 100 μg/ml of proteinase K (Invitrogen Corp.) in PBTS (pH 7.4) for 30 min at 37°C. For $CD2^+$ and $CD3^+$ T-cell antigens, sections were subjected to optimal pressure cooking in 0.01 M citric acid buffer (pH 6.0) for 10 min.

The tissue slides were then washed in PBTS three times and blocked with 1% normal goat serum for 30 min at room temperature. The sections were coated with primary antibodies (all 1:50 in PBTS) and incubated overnight at 4°C. Tissue sections were then washed three times with PBTS, and the secondary antibody, biotinylated goat anti-mouse IgG (1:200; Dako), was incubated with the tissues for 1 h at 37°C. The slides were washed with PBTS before being incubated for 1 h at 37°C with streptavidin-alkaline phosphatase conjugate (1:200; Dako). The sections were then equilibrated with 0.1 M Tris-HCl (pH 8.2) for 5 min at room temperature. The final reaction was produced by immersing sections in a staining solution (1 tablet of Fast Red in 2 ml 0.1 M Tris-HCl [pH 8.2]; Roche Applied Science) for 10 min at room temperature. Sections were counterstained with Mayer's hematoxylin. The $CD2^+$, $CD3^+$, $CD4^+$, and $CD8^+$ antigen-positive scores were computed by estimating the distribution and number of antigen-positive cells in the lung sections per microscopic area (at magnification ×300) based on the following criteria: 0, no positive cells; 1, minimal staining (less than 10 positive cells, with focal or multifocal staining); 2, moderate staining (from 11 to 25 positive cells, with focal or multifocal staining); 3, moderately high staining (from 26 to 50 positive cells, with multifocal or diffuse staining); and 4, high staining (more than 50 positive cells, with diffuse staining).

ELISPOT assay for gamma interferon (IFN-γ)-secreting cells in TBLNs. For the isolation of mononuclear cells (MNC), the TBLNs were collected from euthanized pigs and processed as previously described (53). A cytokine enzyme-linked immunospot (ELISPOT) assay for IFN-γ was conducted as follows: Multiscreen-IP sterile 96-well plates (Millipore, Bedford, MA) were coated with 100 μl of anti-porcine IFN-γ (5 μg/ml) (Biosource, Camarillo, CA), overnight at room temperature. Prior to use, the plates were blocked with RPMI 1640 medium containing 8% fetal bovine serum for 2 h at room temperature, and then cell suspensions were added in duplicate wells at concentrations of 5×10^5 and 5×10^4 cells per well. Cells were stimulated with 50 μg/ml of clarified PRCV or 10 μg of phytohemagglutinin (positive control) or RPMI (negative control). The optimal time and dose for in vitro antigen restimulation were determined in preliminary experiments. After 72 h of incubation at 37°C with 5% CO_2, the cells were washed and 100 μl of biotinylated MAb to porcine IFN-γ (1 μg/ml) (Biosource) was added. Plates were incubated overnight at 4°C. Horseradish peroxidase-conjugated streptavidin (Biosource) was added in 100 μl at a concentration of 0.3 μg/ml, and plates were incubated for 2 h at room temperature. The spots were developed with H_2O_2 and 3-amino-9-ethylcarbazole (Sigma-Aldrich, St. Louis, MO). Cytokine-secreting cells (CSC) were counted using an ImmunoSpot series 3A analyzer (Cellular Technology, Ltd., Cleveland, OH) and expressed as numbers of CSC per 5×10^5 MNC. The background cytokine production reflecting in vivo residual stimulation was assessed by stimulating cells with only RPMI medium; these cell counts were subtracted from the PRCV-stimulated CSC.

Statistical analysis. All values are expressed as the means ± standard errors of the means (SEM). Data among four treatment groups (PRCV/PBS, PRCV/DEX, mock/PBS, and mock/DEX) were analyzed and compared by the Kruskal-Wallis test (nonparametric) using the Statistical Analysis Systems software (SAS Institute, Inc., Cary, NC). A P value of <0.05 was considered statistically significant. Fischer's exact test was used to evaluate the proportion of pigs with RT-PCR-positive nasal swabs between the PRCV/PBS and PRCV/DEX-treated groups.

RESULTS

Mild clinical response to PRCV infection and corticosteroid (DEX) treatment. Clinical signs in PRCV/PBS and PRCV/DEX pigs ranged from sneezing to coughing, mild fever (the average rectal temperature was between 39.6°C and 40.0°C), mild polypnea (respiratory rate of ≥60 movements per min), and anorexia, whereas mock/DEX pigs had mild anorexia throughout the experiment and no clinical signs were observed in mock/PBS control pigs. No significant differences in the amount of sneezing and coughing between PRCV/PBS pigs, PRCV/DEX pigs, and the two control groups were observed (data not shown). The PRCV/DEX pigs showed small increases in rectal temperatures and respiratory rates at PID 4, 6, and 8 compared to rates for PRCV/PBS pigs, although these changes were not statistically significant between the two groups. The PRCV/PBS-, PRCV/DEX-, and mock/DEX-treated pigs had decreased rates of body weight gain from PID 10 to PID 21 compared to those for mock/PBS pigs, but the differences among the four groups were not statistically significant.

Gross and histologic lesions of PRCV/DEX pigs were milder earlier, at PID 2, but more severe later, at PID 4, 10, and 21, than those of PRCV/PBS pigs. Gross lesions of PRCV/PBS and PRCV/DEX pigs were limited to the lungs and TBLNs. Gross lung lesions were characterized by multifocal to coalescing reddish-tan consolidation of the lung, especially involving the cranial lobes. The TBLNs of PRCV/PBS and PRCV/DEX pigs were enlarged and mildly congested from PID 2 to PID 21 compared results for to mock/PBS and mock/DEX control pigs (Fig. 1A). No macroscopic lung lesions were present in mock/PBS control pigs (22/23), but one of the mock/PBS pigs at PID 4 had histologically mild interstitial pneumonia and focal atelectasis. On the other hand, the mock/DEX pigs (12/25; 48%) had mild to moderate focal pneumonic lesions in 1/5 pigs at PID 2, 3/5 pigs at PID 4, 3/5 pigs at PID 8, 4/4 pigs at PID 10, and 1/6 pigs at PID 21. The LN/BW ratios, used to evaluate

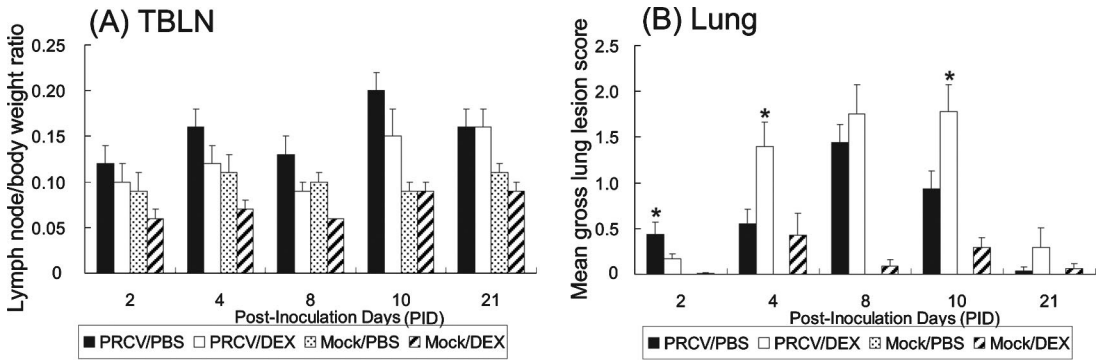

FIG. 1. Mean LN/BW ratios (A) and gross lung lesion scores (B) for the four experimental pig groups at different PID: $n = 4$ to 5 at PID 2 and 10, $n = 5$ at PID 4 and 8, and $n = 5$ to 6 at PID 21 for mock/PBS and mock/DEX groups; $n = 8$ at PID 2 to 10 and $n = 9$ at PID 21 for PRCV/PBS and PRCV/DEX groups. (A) The left TBLNs from each pig were weighed, and the LN/BW ratios of the lymph nodes were calculated. The left TBLNs of mock/DEX and PRCV/DEX pigs were atrophic by 60 to 80% at PID 2, 4, 8, and 21 and 69 to 83% at PID 2, 4, 8, and 10 compared to those of mock/PBS and PRCV/PBS pigs, respectively. However, the differences in LN/BW ratios were not statistically significant (Kruskal-Wallis test) due to animal variability. (B) Gross lung lesions were evaluated based on the percentage of virus-induced lesions (consolidation) of all six lobes. PRCV/DEX pigs had significantly milder lesions than PRCV/PBS pigs at PID 2. However, at PID 4 and 10, the percentages of overall lung tissue consolidation were significantly higher for PRCV/DEX pigs than for PRCV/PBS pigs. Each bar represents the mean ± SEM. An asterisk above a bar represents significant differences ($P < 0.05$) between results for PRCV/PBS and PRCV/DEX pigs by the Kruskal-Wallis test.

enlargement of the lymph nodes, indicated that the left TBLNs of mock/DEX and PRCV/DEX pigs were atrophic by 60 to 80% at PID 2, 4, 8, and 21 and by 69 to 83% at PID 2, 4, 8, and 10 compared to those of mock/PBS and PRCV/PBS pigs, respectively. However, the differences in LN/BW ratios between each of the two groups were not statistically significant (Kruskal-Wallis test) (Fig. 1A). These findings indicate a degree of immunosuppression in DEX-treated pigs which might be associated with the mild pulmonary lesions observed in mock/DEX pigs (but much less severe than those in the PRCV/PBS and PRCV/DEX pigs).

Gross lung lesions in pigs receiving PRCV without DEX treatment were mild at PID 2 and 4, severe at PID 8, moderate at PID 10, and nearly resolved at PID 21, whereas PRCV/DEX-treated pigs had lesions that were mild at PID 2, severe at PID 4, 8, and 10, and mild at PID 21 (Fig. 1B). The PRCV/DEX pigs had significantly milder lesions than the PRCV/PBS pigs at PID 2 ($P < 0.05$), However, at PID 4 and 10, the percentages of overall lung tissue consolidation for PRCV/DEX pigs were significantly higher than those for the PRCV/PBS pigs ($P < 0.05$) (Fig. 1B).

Histological lesions of PRCV/PBS and PRCV/DEX pigs were limited to the lungs and TBLNs. The changes in histological lung lesions were consistent with the macroscopic lung pathology. TBLNs were mildly hyperplastic from PID 2 to PID 21 for PRCV/PBS and PRCV/DEX pigs compared to results for mock/PBS and mock/DEX control pigs. No significant lung lesions (moderate to severe interstitial pneumonia or bronchopneumonia) and lymphoid depletions were present in any of the tissues from mock/PBS and mock/DEX pigs from PID 2 and PID 21 (see Fig. 3A), but mild focal interstitial pneumonia was frequently observed. The PRCV/PBS and PRCV/DEX pigs developed interstitial pneumonia characterized by the following: (i) thickening of the alveolar septa by infiltration of inflammatory leukocytes, principally mononuclear cells (see Fig. 3E and G); (ii) type 2 pneumocyte hypertrophy and hyperplasia (see Fig. 3E and G); (iii) accumulation of necrotic cells and inflammatory leukocytes in alveolar and bronchiolar lumina due to airway epithelial necrosis (see Fig. 3B and C); and (iv) peribronchiolar or perivascular lymphohistiocytic inflammation (see Fig. 3D). Interstitial pneumonia in pigs receiving PRCV alone was first observed at PID 2, peaked in severity at PID 8, and was nearly resolved at PID 21, whereas PRCV/DEX pigs had mild lesions at PID 2 but severe lesions at PID 4, 8, and 10 and mild lesions by PID 21 (Fig. 2). The PRCV/PBS pigs had significantly higher lesion scores than the PRCV/DEX pigs at PID 2 but with the opposite effect at PID 4 and at PID 21 for the PRCV/DEX pigs (Fig. 2). In particular, at PID 4, PRCV/DEX pigs had more-severe bronchointersti-

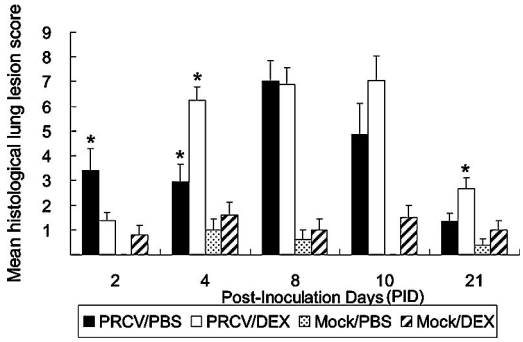

FIG. 2. Mean histological lung lesion scores for the four experimental pig groups at different PID with numbers of pigs at each time point as indicated in the legend to Fig. 1. Histological lung lesion scores ranged from 0 (no abnormalities) to 12 (most severe) based on the combined score of three parameters: (i) thickening of the alveolar septa (0 to 6); (ii) accumulation of necrotic cells and inflammatory leucocytes in alveolar and bronchiolar lumina (0 to 3); and (iii) peribronchiolar or perivascular lymphohistiocytic inflammation (0 to 3). PRCV/PBS pigs had significantly higher histological lesion scores than PRCV/DEX pigs at PID 2 (*), with the opposite effect at PID 4 (**) and 21 (*). A higher lesion score was also observed at PID 10 for PRCV/DEX pigs. Each bar represents means ± SEM. *, $P < 0.05$; **, $P < 0.01$ (asterisk[s] above bar represents significant differences between results for PRCV/PBS and PRCV/DEX pigs by the Kruskal-Wallis test).

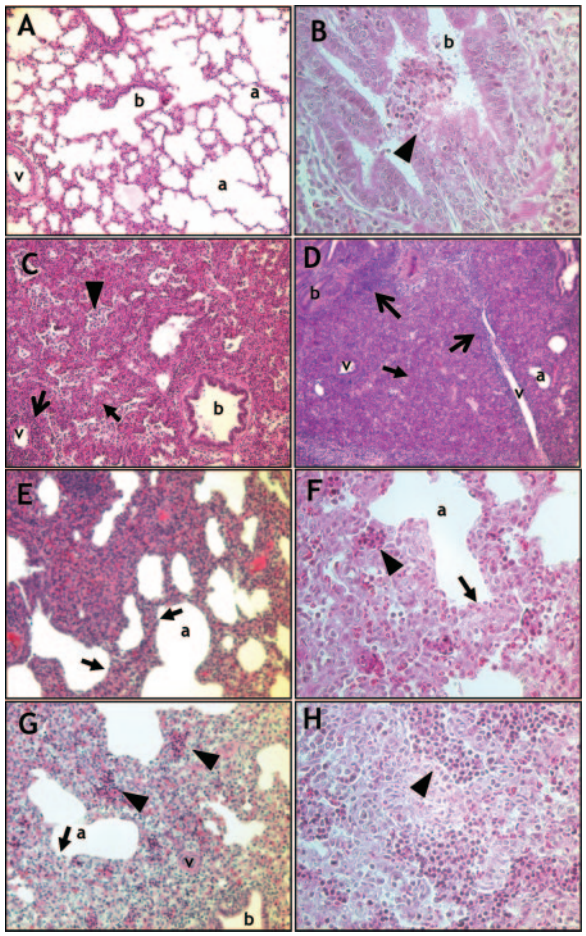

FIG. 3. Lung histopathology. Histopathological lesions in the lungs of mock-infected pigs (A) or PRCV-infected pigs with (C, D, G, and H) or without (B, E, and F) DEX treatment. Note that the lungs of PRCV/DEX-treated pigs had more-severe bronchopneumonia than those of PRCV/PBS-treated pigs at PID 4. (A) Mock/PBS-treated control at PID 4. No abnormalities; original magnification, ×100. (B) PRCV/PBS pig at PID 2 showing moderate to severe diffuse necrosis of the bronchiolar epithelium, with the presence of necrotic cells with pycnotic and karyorrhectic nuclei and exfoliated epithelial cells (arrowhead) in the lumen; original magnification, ×300. (C) PRCV/DEX pig at PID 4 showing moderate diffuse bronchointerstitial pneumonia characterized by the thickening of alveolar septa with type 2 pneumocyte hyperplasia and inflammatory leucocytes such as alveolar macrophages and lesser lymphocytes (solid-headed arrow), accumulation of inflammatory cells (alveolar macrophages and lesser lymphocytes), desquamated epithelial necrotic cells (arrowhead), and perivascular lymphohistiocytic inflammation (open-headed arrow); original magnification, ×100. (D) PRCV/DEX pig at PID 10 showing severe diffuse bronchointerstitial pneumonia with severe peribronchiolar and perivascular lymphohistiocytic inflammation. Note that normal alveolar spaces were rarely observed throughout the pulmonary parenchyma; original magnification, ×50. (E) PRCV/PBS pig at PID 4 showing mild to moderate thickening of the alveolar septa (solid-headed arrow) with mild to moderate type 2 pneumocyte hyperplasia and macrophage infiltration; original magnification, ×150. (F) PRCV/PBS pig at PID 4 (higher magnification of panel E) showing mild to moderate thickening of alveolar septa (solid-headed arrow) and alveolar spaces containing small amounts of cellular debris and mononuclear cells (arrowhead); original magnification, ×300. (G) PRCV/DEX pig at PID 4 showing alveolar septa markedly thickened by type 2 pneumocyte hyperplasia and hypertrophy and by infiltrates of alveolar macrophages (solid-headed arrow). Alveolar spaces contain larger amounts of cellular debris and mononuclear cells (arrowhead) than observed for the PRCV/PBS pigs; original magnification, ×200. (H) PRCV/DEX pig at PID 4 (higher magnification of panel G) showing alveolar spaces containing larger amounts of cellular debris and mononuclear cells (arrowhead) than was the case for the PRCV/PBS pigs; original magnification, ×300. Hematoxylin and eosin stain was used. a, alveolar space; b, bronchiolar lumen; v, pulmonary blood vessel.

tial pneumonia than PRCV/PBS pigs (Fig. 3E, F, G and H). One of the three major histological changes, perivascular and peribronchiolar lymphohistiocytic inflammation, was observed at PID 2, 4, 8, and 10 (Fig. 3D). Decreased perivascular and peribronchiolar lymphohistiocyte cuffing in the lungs of PRCV/DEX pigs was observed at PID 4 and 8 compared to results for the PRCV/PBS pigs, although the differences between the two groups were not significant (Kruskal-Wallis test).

To summarize the gross and histological lung findings, the PRCV/DEX pigs developed pulmonary lesions that were milder at the beginning of the infection (PID 2). However, maximal pulmonary lesions were observed within 4 days after PRCV and DEX treatment, whereas PRCV/PBS pigs did not develop maximum lesions until 8 days postinoculation. Although the pneumonic lesions of the PRCV/PBS pigs were moderate at PID 10 and were almost resolved at PID 21, the pneumonic lesions in PRCV/DEX pigs continued to be severe through PID 10 and persisted in a mild form through PID 21.

Lungs of PRCV/DEX pigs had lower numbers of PRCV antigen-positive cells at PID 2 but higher numbers at PID 4, 10, and 21 than PRCV/PBS pigs. The IHC-positive staining for PRCV was identified as an intense brown intracytoplasmic reaction and was limited to lung tissues. The distribution of PRCV antigens was closely related to the histopathological lesions and did not differ between PRCV/PBS and PRCV/DEX pigs. At the beginning of infection (PID 2), most PRCV antigens, in decreasing order of frequency, were found in bronchial and bronchiolar epithelium with numerous necrotic cells in the lumen (shown in Fig. 4B and C), type 2 pneumocytes (shown in Fig. 4E and F), and other pulmonary cells, such as alveolar macrophages (shown in Fig. 4D) and type 1 pneumocytes. By PID 4, 8, and 10, PRCV antigen-positive cells in bronchioles were rare and the majority of IHC-stained cells (>70%) were type 2 pneumocytes (Fig. 4E). Most of the PRCV-positive cells were hypertrophied type 2 pneumocytes in a single line pattern within the thickened alveolar septa (Fig. 4E and F). At PID 21, when the lesions were almost resolved, the overall number of PRCV antigen-positive cells was low but was markedly increased for alveolar macrophages relative to results at previous time points, indicating that the type 2 pneumocyte hyperplasia caused by the PRCV infection was decreasing and the phagocytic alveolar macrophages that engulf PRCV-infected cells were increased. The IHC results confirmed that the major infected cell type in the lungs of PRCV-infected pigs consists of alveolar epithelial cells and specifically type 2 pneumocytes. None of the lungs or other organs from mock/PBS and mock/DEX pigs showed IHC staining for PRCV antigen.

The time sequence of changes in PRCV antigen-positive scores was similar to those for the degrees of gross and histopathological lung lesions (Fig. 1B, 2, and 4G). The PRCV

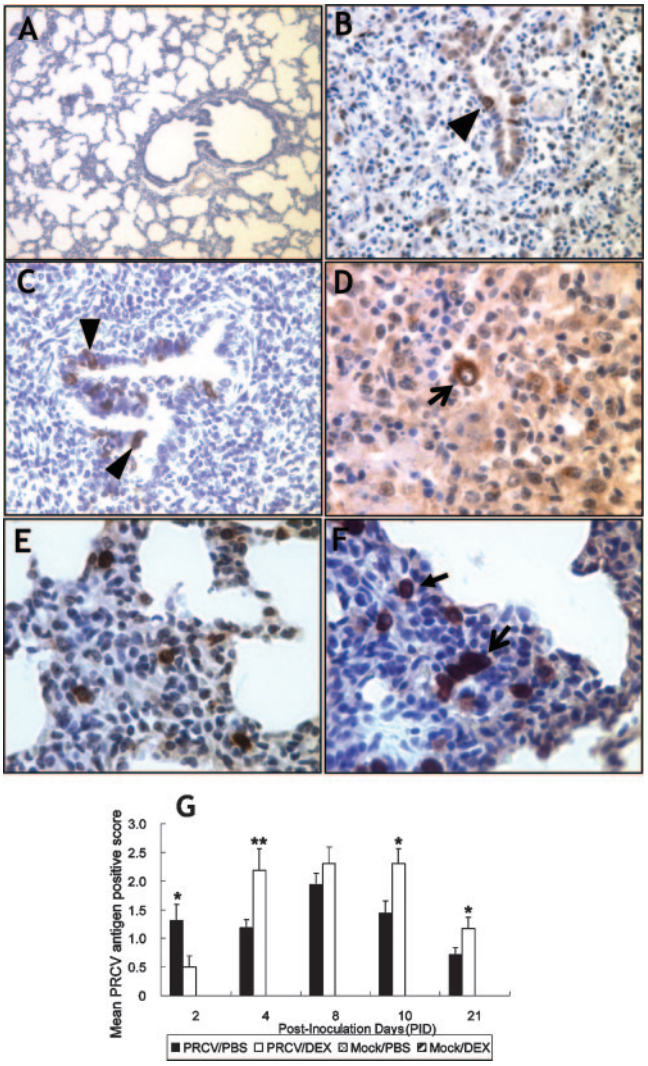

FIG. 4. Localization of PRCV antigens (A to F) and IHC staining scores (G) in the lungs of pigs in the four experimental groups. (A) Mock/PBS-treated control pig at PID 4. No positive cells evident; original magnification, ×100. (B) Pig in PRCV/PBS group at PID 4. The PRCV antigen (brown stain; arrowhead) was observed in a few scattered bronchiolar epithelial cells with markedly thickened alveolar septa; original magnification, ×200. (C) Pig in PRCV/DEX group at PID 4. Note high numbers of PRCV antigen-positive (arrowheads) bronchiolar epithelial cells; original magnification, ×200. (D) Pig in PRCV/PBS group at PID 10. The PRCV antigen (open-headed arrow) was occasionally observed in interstitial macrophages within the thickened alveolar septa; original magnification, ×400. (E) Pig in PRCV/PBS group at PID 10. PRCV antigen-positive cells were scattered within the mild thickened alveolar septa; original magnification, ×400. (F) Pig in PRCV/DEX group at PID 10. PRCV antigens were found in hypertrophied type 2 pneumocytes in a single line pattern (open-headed arrow) and in alveolar macrophage-like mononuclear cells (solid-headed arrows) within the thickened alveolar septa. For PRCV/DEX pigs, numbers of PRCV antigen-positive cells were higher than those for PRCV/PBS pigs (E) at the same time; original magnification, ×400. IHC, 3,3′-diaminobenzidine, and Mayer's hematoxylin counterstain were used (G) IHC staining scores at each PID with pig numbers at each time indicated as described in the legend to Fig. 1. PRCV antigen-positive scores were computed by estimating the number of PRCV-positive cells in the lung by the following criteria: 0, no positive cells; 1, few (less than 10 positive cells); 2, moderate (from 11 to 25 positive cells); and 3, high (more than 26 positive cells). Note that PRCV/DEX pigs had significantly lower numbers of PRCV antigen-positive cells than PRCV/PBS pigs at PID 2 (*). In contrast, at PID 4 (**) and PID 10 and 21 (*), numbers of PRCV antigen-positive cells were significantly higher for PRCV/DEX pigs. Each bar represents means ± SEM. *, $P < 0.05$; **, $P < 0.01$ (asterisk[s] above bar represents significant differences between PRCV/PBS and PRCV/DEX pigs by the Kruskal-Wallis test).

antigen-positive scores peaked at PID 8 (like the lesion scores) in the PRCV/PBS group, but in the PRCV/DEX pigs, the PRCV antigen-positive and lesion scores peaked at PID 4 to 10. At PID 2, the PRCV/DEX pigs had significantly fewer numbers of PRCV antigen-positive cells than PRCV/PBS pigs (Fig. 4G). In contrast, at PID 4, 10 and 21, the PRCV/DEX pigs had significantly higher numbers of PRCV antigen-positive cells, which also corresponded to the more-severe pneumonic lesions for the PRCV/DEX pigs than for the PRCV/PBS pigs at PID 4, 10, and 21.

Nasal shedding of PRCV and viral titers did not differ between PRCV/PBS and PRCV/DEX pigs. There were no significant differences (Kruskal-Wallis test) in patterns of nasal shedding of PRCV in the upper respiratory tract and viral titers at each PID between PRCV/PBS and PRCV/DEX pigs as determined by CCIF and real-time PCR (data not shown). These data suggest that the pigs infected with 1×10^7 PFU of PRCV, with or without DEX, did not show substantial differences in nasal virus titers and shedding kinetics. Such differences in nasal shedding may be more obvious at lower initial infectious doses of inoculum (28). In addition, the large variability in values at each PID among the outbred pigs in the different experimental trials likely compromised the power to detect differences. The highest mean PRCV titers were $10^{6.6}$ FFU/ml for both PRCV/PBS pigs and PRCV/DEX pigs at PID 2, and titers decreased progressively thereafter (data not shown). Similar to the CCIF results, real-time PCR showed that the highest mean titers were $10^{3.6}$ PFU per ml (PFU/ml) for PRCV/PBS pigs and $10^{3.0}$ PFU/ml for PRCV/DEX pigs at PID 2 and also decreased progressively thereafter (data not shown). The duration of nasal shedding was 10 and 12 days for both infected groups by CCIF and real-time PCR, respectively.

No significant differences (Fischer's exact test) in percentages of PRCV-positive pigs were observed between PRCV/PBS and PRCV/DEX pigs as determined by one-step RT-PCR assays, although differences at PID 6, 8, and 10 were observed. In the nasal samples from PRCV/PBS pigs, nasal shedding of PRCV was identified for 0/37 (0%) at PID 0, 36/36 (100%) at PID 2, 26/28 (93%) at PID 4, 22/25 (88%) at PID 6, 17/23 (77%) at PID 8, 6/12 (50%) at PID 10, and 0/28 (0%) between PID 12 and PID 21. For PRCV/DEX pigs, nasal shedding of PRCV was detected for 0/37 (0%) at PID 0, 36/36 (100%) at PID 2, 26/28 (93%) at PID 4, 23/25 (92%) at PID 6, 19/23 (83%) at PID 8, 7/12 (58%) at PID 10, and 0/28 (0%) between PID 12 and PID 21. No nasal shedding of PRCV was detected for the mock/PBS pigs and mock/DEX pigs between PID 0 and PID 21.

PRCV/DEX pigs had greater or significantly greater amounts of PRCV RNA in the lungs and BAL fluids at PID 4, 8, 10, and 21, with lower viral RNA titers at PID 2. In contrast to results for the upper respiratory tract, significant differences

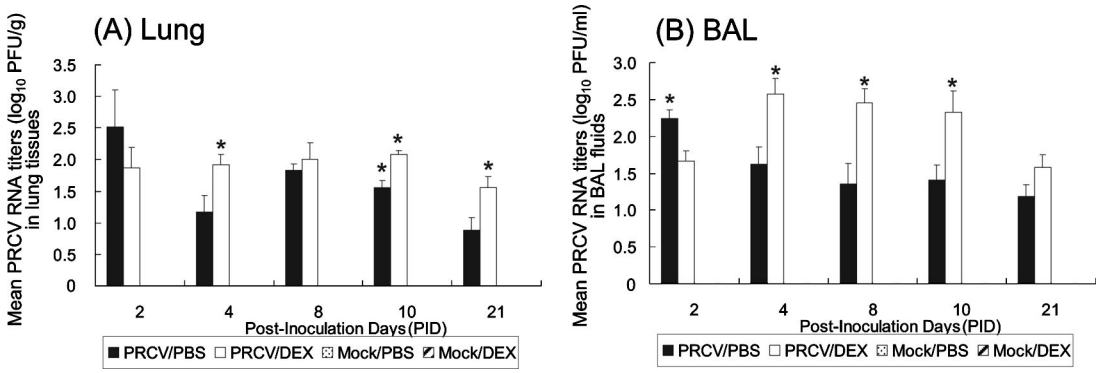

FIG. 5. Mean PRCV RNA titers as determined by real-time RT-PCR in lung tissues (A) and BAL fluids (B). The four experimental pig groups were examined at the indicated PID, with pig numbers at each time as indicated in the legend to Fig. 1. Mean viral RNA titers were expressed as log_{10} PFU per gram of lung tissue or log_{10} PFU per ml of BAL fluid. (A) Lungs of PRCV/PBS pigs had higher (1.35-fold) viral RNA levels than those of PRCV/DEX pigs at PID 2 but with the opposite effect at PID 4 (*), 10 (*), and 21 (*), with significantly higher viral RNA levels for PRCV/DEX pigs. (B) BAL fluids of PRCV/PBS pigs had significantly higher viral RNA levels than PRCV/DEX pigs at PID 2 (*) but with the opposite effect at PID 4, 8, and 10 (*), with significantly higher viral RNA levels for the PRCV/DEX pigs and 1.33-fold higher levels also at PID 21. Each bar represents the mean ± SEM. *, $P < 0.05$; **, $P < 0.01$; an asterisk(s) above a bar represents significant differences between PRCV/PBS and PRCV/DEX pigs as determined by the Kruskal-Wallis test.

in PRCV RNA titers in the lung homogenates and BAL fluids were identified between PRCV/PBS and PRCV/DEX pigs. No PRCV-positive lung homogenate and BAL fluid samples were detected in the mock/PBS and mock/DEX control pigs by either real-time RT-PCR or one-step RT-PCR. In the homogenized lung samples, peak viral RNA titers of $10^{2.5}$ PFU per gram were observed for PRCV/PBS pigs at PID 2 and $10^{2.0}$ PFU/g for PRCV/DEX pigs at PID 8 and 10. Mean viral RNA titers in the lung samples from PRCV/DEX pigs were significantly higher than those in samples from PRCV/PBS pigs at PID 4 ($P < 0.05$), 10 ($P < 0.01$), and 21 ($P < 0.05$) (Fig. 5A), indicating that DEX treatment enhanced PRCV replication in the lung. In the BAL fluid samples, peak viral RNA titers were $10^{2.2}$ PFU/ml for PRCV/PBS pigs at PID 2 and $10^{2.5}$ PFU/ml for PRCV/DEX pigs at both PID 4 and 8. At PID 2, the viral RNA titer ($10^{1.7}$ PFU/ml) in the BAL of PRCV/DEX pigs was significantly lower than that for PRCV/PBS pigs ($10^{2.2}$ PFU/ml) ($P < 0.05$) (Fig. 5B). However, at PID 4, 8, and 10 (all $P < 0.05$), viral RNA titers for the PRCV/DEX pigs were significantly higher (40- to 63-fold) than those for the PRCV/PBS pigs, consistent with the changes in the PRCV antigen-IHC scores.

Lungs of PRCV/DEX pigs had fewer $CD2^+$, $CD3^+$, $CD4^+$, and $CD8^+$ T cells at PID 8 and 10 than PRCV/PBS pigs. The overall time course patterns of T-lymphocyte populations in the lungs of PRCV/PBS pigs were similar to those for PRCV/DEX pigs. However, there were significant differences at PID 4, 8, and 10, when histological changes such as thickening of the alveolar septa and peribronchiolar and perivascular lymphohistiocytic cuffing were most pronounced. The $CD2^+$, $CD3^+$, $CD4^+$, and $CD8^+$ T cells were rarely detected in the lung parenchyma of mock/PBS and mock/DEX pigs, and the differences between these two groups were not statistically significant. In contrast, the lungs of PRCV/DEX pigs had significantly fewer $CD2^+$ T cells at PID 4 and $CD2^+$, $CD3^+$, $CD4^+$, and $CD8^+$, T cells at PID 8 and 10 than the PRCV/PBS pigs (Fig. 6A to D and Fig. 7A to D). The distribution patterns of $CD2^+$ and $CD3^+$ T cells in the lungs were similar to each other for both PRCV-infected groups: they were distributed throughout the thickened lung parenchyma, particularly around the bronchioles and blood vessels with lymphohistiocytic inflammation (Fig. 7A and B). The numbers of $CD4^+$ and $CD8^+$ T cells were less than those of $CD2^+$ and $CD3^+$ T cells in the lungs of both PRCV-infected groups. The immunostaining patterns resembled those of $CD2^+$ and $CD3^+$ T cells (Fig. 7C and D).

Numbers of IFN-γ CSC in TBLNs of PRCV/DEX pigs were lower than those for PRCV/PBS pigs at PID 4, 8, and 10. Mononuclear cells were purified from the TBLNs, and a cytokine ELISPOT assay was used to quantitate Th1 (IFN-γ) CSC after in vitro stimulation of MNC with purified PRCV antigen. The PRCV/PBS pigs showed a trend of increasing IFN-γ CSC in the TBLN from PID 2 to 21. On the other hand, PRCV/DEX pigs did not show any increases between PID 4 and 10, although a mild increase at PID 2 was observed (data not shown). Mock/PBS and mock/DEX pigs had a minimal number (0 to 19.1 CSC/5 × 10^5 MNC) of PRCV-specific IFN-γ CSC throughout the experiment. The number of IFN-γ CSC for PRCV/PBS pigs (91 to 412 CSC/5 × 10^5 MNC) was significantly higher than that for PRCV/DEX pigs (0 to 161.5 CSC/5 × 10^5 MNC) at PID 10; in addition, the PRCV/PBS pigs had higher numbers of IFN-γ CSC than the PRCV/DEX pigs at PID 4 and 8 (data not shown), although the differences between the groups were not statistically significant (Kruskal-Wallis test).

DISCUSSION

Our study was designed to determine whether DEX treatment affects PRCV-induced pneumonia with a porcine model, with the ultimate goal of using the atypical pneumonia in PRCV-infected pigs as a model to mimic SARS-CoV disease in the lung and to investigate the positive or negative effects of corticosteroid treatment. Our results revealed that corticosteroid treatment may be effective for alleviation of pneumonia (pulmonary lesions) and for decreasing viral replication within

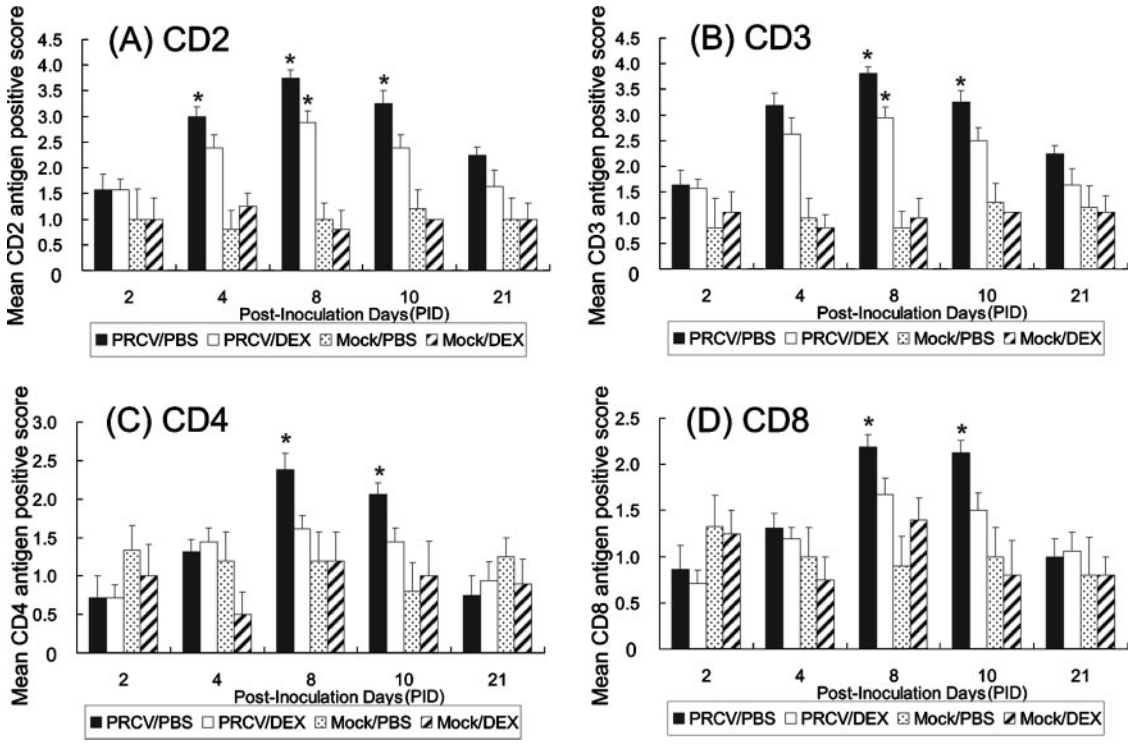

FIG. 6. IHC staining scores of $CD2^+$ (A), $CD3^+$ (B), $CD4^+$ (C), or $CD8^+$ (D) T cells in the lungs of the four experimental pig groups at various PID with pig numbers at each time point as indicated in the legend to Fig. 1. (A and B) Lungs of PRCV/DEX pigs had fewer $CD2^+$ T cells than those of PRCV/PBS pigs at PID 4, 8, and 10 and fewer $CD3^+$ T cells at PID 8 and 10. (C and D) Lungs of PRCV/DEX pigs had fewer $CD4^+$ and $CD8^+$ T cells than those of PRCV/PBS pigs at PID 8 and 10. Each bar represents the mean ± SEM. *, $P < 0.05$; **, $P < 0.01$; asterisk(s) above bar represents significant differences between results for PRCV/PBS and PRCV/DEX pigs as determined by the Kruskal-Wallis test.

the lung early in respiratory CoV infection. However, in the middle and late stages of infection, more-severe pneumonia and extensive viral replication were observed in the lung, likely due to the immunosuppressive effects of the corticosteroid. Corticosteroids, when administered in the early stage of the disease, might alleviate the early inflammation mediated by acute necrosis of bronchiolar and alveolar epithelial cells and reduce the inflammatory response. To our knowledge, this is the first study to examine the effects of corticosteroids on CoV-induced pneumonia in the natural disease host. Some investigators have demonstrated the negative effects of corticosteroids on enteric CoV disease. DEX induced a recrudescence of bovine CoV fecal shedding in bovine CoV-infected cows and more-profuse diarrhea in TGEV-infected pigs than in animals not treated with DEX (45, 52). Considering the milder pneumonic lesions and lower level of viral replication at the beginning of PRCV infections treated with corticosteroids, the appropriate short-term (1 to 2 days) use of corticosteroids may be useful in treatment of acute severe CoV pneumonias, such as SARS-CoV and human CoV-NL63 pneumonias. The latter causes a severe lower respiratory tract disease that occasionally results in death in the aged, who die shortly (5 days) after the onset of disease (2, 54).

In the present study, the corticosteroid regime we used (PID 1 to 6) also reduced the numbers of CD 2^+, $CD3^+$, $CD4^+$ (helper), and $CD8^+$ (cytotoxic) T cells in the pulmonary lesions and TBLNs of PRCV/DEX pigs at the middle stages of infection (PID 4, 8, and 10) and ultimately induced immunosuppression (decreased IFN-γ CSC). We successfully detected $CD2^+$, $CD3^+$, $CD4^+$, and $CD8^+$ T cells in porcine lung tissues using IHC, although the detection sensitivity was reduced by tissue fixation with paraformaldehyde. These results suggest that the corticosteroid treatments, by decreasing T cells, might affect the clearance of PRCV in the lung, thereby creating an environment for more-extensive viral replication, principally in type 2 pneumocytes with hyperplasia and hypertrophy. At PID 8 and 10, PRCV antigens were frequently detected in hypertrophied type 2 pneumocytes of the thickened alveolar septa. The number of helper T cells and especially cytotoxic T cells present in the thickened alveolar septa could be associated with the clearance of PRCV-infected pneumocytes. In addition, we observed that PRCV-infected, DEX-treated pigs had markedly atrophic TBLNs from PID 2 to PID 10 compared to those of PRCV-infected pigs which did not receive DEX treatment, consistent with the immunosuppressive effects of DEX treatment as determined by both IHC for the profile of T-cells and ELISPOT assay for IFN-γ CSC. The decreased T-cell infiltration into the lung may be directly associated with the reduction of antiviral activity of IFN-γ derived from activated T cells and secondary effects on other inflammatory cells, such as macrophages, monocytes, and neutrophils, as well as endothelial cells and fibroblasts. This decreased cellular immune response in the lungs likely affected viral clearance in the lung and exacerbated the PRCV pneumonia later (at PID 4, 10, and 21) (Fig. 1 and 2). Moreover, the corticosteroid treatments shortened the time to reach the maximum pulmonary lesion.

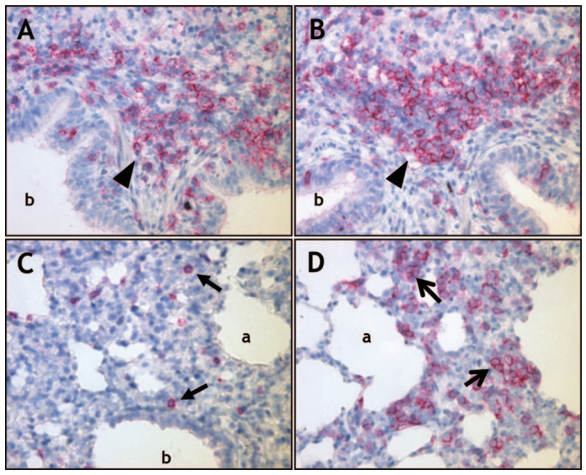

FIG. 7. Distribution and localization of T cells in lungs of PRCV-infected pigs with or without DEX treatment at PID 8. (A) Pig in PRCV/DEX group, stained with anti-CD3 serum. A number of $CD3^+$ T-cells (red stain; arrowhead) were observed around the bronchioles and were scattered within the bronchiolar epithelium; original magnification, ×200. (B) Pig in PRCV/PBS group, stained with anti-CD3 serum. Higher numbers of $CD3^+$ T cells (arrowhead) were observed around the bronchioles and were scattered within the bronchiolar epithelium than was the case with the PRCV/DEX pigs at the same time point; original magnification, ×200. (C) Pig in PRCV/DEX group stained with anti-CD8 serum. A few $CD8^+$ T cells (solid-headed arrows) were scattered within the moderately thickened alveolar septa; original magnification, ×200. (D) Pig in PRCV/PBS group stained with anti-CD8 serum. Higher numbers of $CD8^+$ T cells (open-headed arrows) were observed within the mildly to moderately thickened alveolar septa than was the case with the PRCV/DEX pigs at the same time point; original magnification, ×200. IHC, alkaline phosphatase, red substrate, and Mayer's hematoxylin counterstain were used.

Our study suggests that corticosteroids could also alter the pathogenesis of SARS-CoV in the human lung in a similar manner. In our study, the daily consecutive treatments with high-dose corticosteroid contributed to the more rapid development of maximal PRCV pneumonic lesions and to a longer course of severe pneumonia (Fig. 1B and 2). Moreover, the pulmonary lesions in DEX-treated animals took longer to resolve than those in untreated animals. For SARS-CoV, severe pneumonic lesions are associated with continued tissue damage induced potentially by a hyperimmune response of activated inflammatory cells, such as macrophages and cytotoxic $CD8^+$ T cells, within the lesion (5). For SARS-CoV, the longer the pneumonia persisted the more severe the pneumonia became, and the prognosis of the patient worsened. Cameron et al. recently reported that corticosteroids may preclude SARS-CoV clearance from the lungs of patients during the acute phase of SARS by downregulating proinflammatory gene expression, thereby potentially decreasing antiviral alpha interferon and IFN-γ plasma levels, as determined by microarray analysis and cytokine assay (6). The authors further proposed that corticosteroid treatment may disrupt the homeostatic regulation of innate and adaptive immune responses in SARS patients. The unproven long-term and high-dose application of corticosteroids to SARS patients during the outbreak might similarly exacerbate SARS-CoV pneumonia and extend the recovery phase of the disease by inducing prolonged immunosuppression, leading to reduced cellular immunity within the lung as found in our study.

Corticosteroids are commonly used to alleviate excessive immune responses in autoimmune disease and to reduce inflammation caused by viral or bacterial infections. In the initial stages of infection, SARS-CoV significantly increased serum levels of alpha interferon and IFN-γ and the chemokines CXCL10 and interleukin 8 (IL-8) in SARS patients, concomitant with a decrease in levels of IL-12p70, IL-2, and tumor necrosis factor alpha (TNF-α) (5). The decreased serum TNF-α is in opposition to its marked increase in avian influenza H5N1 infections, which show lung pathology similar to that of SARS-CoV (5, 34). In avian influenza H5N1 pneumonia in humans, macrophage inflammation is dominant in the early stages of the infection and the stimulated macrophages release proinflammatory cytokines, such as TNF-α. Macrophage infiltration in SARS pneumonia is speculated to play a lesser role in the pathogenesis of SARS than is the case with H5N1 infections (5, 34). The regimen of corticosteroid treatments used for SARS patients and the clinical outcomes have been reviewed (14). Low-dose corticosteroids, such as 0.5 to 1.0 mg/kg per day for prednisolone, have been used to treat common infections and for acute respiratory distress syndrome, a term which is used to describe severe acute lung failure resulting from diverse causes. However, for SARS, approximately 10- to 20-fold-higher doses of corticosteroids were administered intravenously or orally to patients (1, 14, 27). Clinicians initially prescribed intravenous hydrocortisone at 400 to 800 mg/day (or 8 to 12 mg/kg/day, intravenous) or methylprednisolone at 60 to 80 mg/day (or 1 to 3 mg/kg/day, intravenous) and alternatively used pulsed intravenous methylprednisolone at 500 to 1,000 mg/day of treatment if the condition of the SARS patient worsened (1, 14, 27). Although human clinical data on the effects of corticosteroids on viral pneumonias are limited, low-dose and short-term (1 to 2 days) corticosteroid (DEX) treatments have been shown to be effective against human respiratory syncytial virus in rats when administered in a single daily intraperitoneal dose of 0.6 or 1.2 mg/kg and against varicella pneumonia in humans who received 800 mg/day of hydrocortisone for 2 days (33, 38).

Recently clinicians have emphasized the potential risks in the use of corticosteroids for SARS patients, because patients receiving the treatment ultimately had serious adverse effects, such as fatal secondary viral/fungal/bacterial infections due to the immunosuppressive effects (1, 7, 13, 15, 18, 21, 22, 31, 36, 56). One study reported that in a total of 20 clinical cases, pulmonary aspergillosis was prevalent (10%) in fatal SARS infections in patients given high-dose corticosteroids (22). The main causative agent of fungal pulmonary infections, *Aspergillus* spp., is an opportunistic pathogen in immunocompromised or debilitated patients. Additionally, SARS-CoV infection may directly predispose patients to develop concurrent secondary infections, similar to the observation that secondary bacterial or mycoplasmal infections are frequent in pigs with PRCV or PRRSV pneumonia (35, 44). The mechanism, however, is unclear (35). Some reports have indicated that the lungs of SARS patients treated with high-dose corticosteroids have fewer $CD3^+$ T cells and $CD20^+$ B cells than those of untreated patients, demonstrating the compromised immune condition of the patients (3). Moreover, the significant lymphopenia ob-

served in SARS patients was associated with the use of corticosteroids (58). These reports support the immunosuppressive effects of the corticosteroid treatments and are consistent with the outcomes in the present study.

SARS is an acute lower respiratory tract disease of humans, causing severe necrosis of bronchiolar and alveolar epithelial cells together with type 2 pneumocyte hyperplasia. SARS-CoV pneumonia is characterized by an "atypical pneumonia" with several distinct histological characteristics (8, 11, 13, 22, 34, 35, 51): (i) severe diffuse alveolar damage (DAD) causing hyaline membrane formation in alveolar spaces and interstitial edema, (ii) severe bronchiolar injury to ciliated and nonciliated bronchiolar epithelial cells, and (iii) interstitial pneumonia with type 2 pneumocyte hyperplasia and hypertrophy and multinucleated giant cells, likely originating from pneumocytes. A variety of animal models, including nonhuman primates (macaque and marmoset), ferrets (*Mustela furo*), domestic cats, Golden Syrian hamsters, and BALB/c mice, have been used to study SARS-CoV pathogenesis, and some of these animal models have reproduced some SARS-like symptoms and histopathological lesions. The pulmonary histological lesions in SARS-CoV-infected nonhuman primates, ferrets, and cats but not the rodent species with asymptomatic SARS infection resemble one another, showing interstitial pneumonia, multinucleated epithelial giant cells, type 2 pneumocyte hyperplasia, interstitial edema, and perivascular or peribronchiolar inflammatory cell infiltration but rarely hyaline membrane formation (10, 40, 57). Rodent models seem less robust for the study of SARS-CoV pathogenesis with respect to pneumonia and histopathology, in that pneumonia in mice with SARS-CoV infections includes acute-phase lesions such as necrosis of bronchiolar epithelial cells and hyaline membrane formation due to damage of vascular endothelial cells rather than a proliferative phase characterized by thickening of alveolar septa with type 2 pneumoctye hyperplasia and hypertrophy (10, 40, 57). The cellular tropism of SARS-CoV for bronchiolar and alveolar epithelial cells in mice is distinct from that of SARS-CoV which has a cellular tropism toward type 2 pneumoctyes (8, 10, 40). Moreover, animal models directly using SARS-CoV infections, which require adequate laboratory supervision and facilities with biosafety level 3, have potential risks of laboratory-acquired virus exposure and a new SARS epidemic.

Due to its close physiological, anatomical, and immunological resemblance to humans, the pig is an important model for biomedical research in such areas as human enteric diseases (43). Unlike the case with inbred mouse models, the broad clinicopathological manifestations in outbred pigs are very similar to those in the genetically diverse human population. However, inbred mouse models have been preferred for studying SARS-CoV pathogenesis in spite of their major defects, since they have high rates of reproducibility for histopathological lesions, fatality, and immune responses when large numbers of animals are used (10, 40, 60). However, the pathogenesis of SARS-CoV in mice differs from that in humans in that SARS-CoV causes a more-severe acute infection in mice than in humans and induces high fatality rates, with only rare survivors by 4 days after SARS-CoV infection. In contrast, the mean disease duration for SARS patients who died was longer than 10 days (range, 2 to 20 days) (10, 11, 13, 40, 51, 60). Moreover, the pronounced eosinophilic inflammation observed in the lungs of mice with SARS-CoV infection is not reflective of SARS-CoV-associated pneumonic lesions, and this difference is likely to influence the immune response to SARS-CoV in mice (10, 40, 60). Therefore, by addressing questions that are vital for an understanding of the disease mechanisms of SARS-CoV using PRCV infection in the porcine model to mimic the atypical pneumonia seen in SARS patients, the results may be more directly extrapolated to humans.

SARS-CoV infection stimulates pulmonary epithelial cells and results in cellular proliferation and squamous epithelial metaplasia in the lung, which has also been found in PRCV pneumonia and in porcine reproductive and respiratory syndrome virus infection, which causes interstitial pneumonia and reproductive failure in pigs (9, 17, 35, 42, 44). Our study demonstrates that pneumonic lesions of PRCV in pigs are very similar to SARS-CoV lesions. Like SARS-CoV, PRCV caused the following: (i) severe necrotizing bronchiolitis and alveolitis from the beginning of the infection (PID 2) and occasionally persisting through PID 8 (Fig. 3B and C); (ii) interstitial pneumonia with type 2 pneumocyte hypertrophy and hyperplasia and inflammatory leukocyte infiltration, although mild, from PID 2 through PID 21 (Fig. 2 and 3E to H); and (iii) atypically mild to moderate perivascular and peribronchiolar inflammatory leukocyte infiltration from PID 4 to PID 10 (Fig. 3D). Similar to SARS-CoV pneumonia, inflammatory lesions and a proliferative phase in the lungs of pigs with PRCV infection occurred concurrently in the early and middle stages, from PID 2 to PID 10.

In summary, the present investigation demonstrated an altered pathogenesis of PRCV in the lung due to immunosuppression following treatment with corticosteroids. These results suggest that early limited use of corticosteroids in CoV pneumonia may be effective in reducing the pulmonary lesions and viral replication within the lesions; however, consecutive corticosteroid treatments may shorten the time at which maximum pulmonary lesions develop and may reduce T-cell infiltration into the lung, but concomitantly, viral clearance from the lung may be compromised. Collectively, our results confirm that DEX treatment alleviates PRCV pneumonia early (PID 2) in the infection but exacerbates it at later stages of infection (PID 4, 10, and 21), potentially by decreasing cellular immune responses in the lung (IFN-γ-secreting T cells), thereby creating an environment conducive to more-extensive viral replication. These data have potential implications for corticosteroid use in SARS-CoV disease and suggest a precaution against prolonged, high-dose corticosteroid use.

ACKNOWLEDGMENTS

We thank Juliette Hanson, Greg Meyers, and Todd Root for assistance with animal care and Jeff Hayes (Ohio Department of Agriculture, Reynoldsburg, OH) for helpful suggestions for the pathology studies.

Salaries and research support were provided by state and federal funds appropriated to the Ohio Agricultural Research and Development Center, The Ohio State University. This work was supported by a grant from the National Institute of Allergy and Infectious Diseases, National Institutes of Health, grant R01 AI060739, to the corresponding author (L. J. Saif).

REFERENCES

1. **Auyeung, T. W., J. S. Lee, W. K. Lai, C. H. Choi, H. K. Lee, J. S. Lee, P. C. Li, K. H. Lok, Y. Y. Ng, W. M. Wong, and Y. M. Yeung.** 2005. The use of

cortiocosteroid as treatment in SARS was associated with adverse outcomes: a retrospective cohort study. J. Infect. **51:**98–102.
2. **Bastien, N., K. Anderson, L. Hart, P. Van Caeseele, K. Brandt, D. Milley, T. Hatchette, E. C. Weiss, and Y. Li.** 2005. Human coronavirus NL63 infection in Canada. J. Infect. Dis. **191:**503–506.
3. **Beasley, M. B., T. J. Franks, J. R. Galvin, B. Gochuico, and W. D. Travis.** 2002. Acute fibrinous and organizing pneumonia: a histological pattern of lung injury and possible variant of diffuse alveolar damage. Arch. Pathol. Lab. Med. **126:**1064–1070.
4. **Bohl, E. H., R. K. Gupta, M. V. Olquin, and L. J. Saif.** 1972. Antibody responses in serum, colostrum, and milk of swine after infection or vaccination with transmissible gastroenteritis virus. Infect. Immun. **6:**289–301.
5. **Cameron, M. J., J. F. Bermejo-Martin, A. Danesh, M. P. Muller, and D. J. Kelvin.** 2007. Human immunopathogenesis of severe acute respiratory syndrome (SARS). Virus Res. Doi:10.1016/j.virusres.2007.02.014.
6. **Cameron, M. J., L. Ran, L. Xu, A. Danesh, J. F. Bermejo-Martin, C. M. Cameron, M. P. Muller, W. L. Gold, S. E. Richardson, S. M. Poutanen, B. M. Willey, M. E. DeVries, Y. Fang, C. Seneviratne, S. E. Bosinger, D. Persad, P. Wilkinson, L. D. Greller, R. Somogyi, A. Humar, S. Keshavjee, M. Louie, M. B. Loeb, J. Brunton, A. J. McGeer, Canadian SARS Research Network, and D. J. Kelvin.** 2007. Interferon-mediated immunopathological events are associated with atypical innate and adaptive immune responses in patients with severe acute respiratory syndrome. J. Virol. **81:**8692–8706.
7. **Choi, K. W., T. N. Chau, O. Tsang, E. Tso, M. C. Chiu, W. L. Tong, P. O. Lee, T. K. Ng, W. F. Ng, K. C. Lee, W. Lam, W. C. Yu, J. Y. Lai, S. T. Lai, and the Princess Margaret Hospital SARS Study Group.** 2003. Outcomes and prognostic factors in 267 patients with severe acute respiratory syndrome in Hong Kong. Ann. Intern. Med. **139:**715–723.
8. **Chow, K. C., C. H. Hsiao, T. Y. Lin, C. L. Chen, and S. H. Chiou.** 2004. Detection of severe acute respiratory syndrome-associated coronavirus in pneumocytes of the lung. Am. J. Cin. Pathol. **121:**574–580.
9. **Cox, E., J. Hooyberghs, and M. B. Pensaert.** 1990. Sites of replication of a porcine respiratory coronavirus related to transmissible gastroenteritis virus. Res. Vet. Sci. **48:**165–169.
10. **Deming, D., T. Sheahan, M. Heise, B. Yount, N. Davis, A. Sims, M. Suthar, J. Harkema, A. Whitmore, R. Pickles, A. West, E. Donaldson, K. Curtis, R. Johnston, and R. Baric.** 2006. Vaccine efficacy in senescent mice challenged with recombinant SARS-CoV bearing epidemic and zoonotic spike variants. PLoS Med. **3:**e525.
11. **Ding, Y., H. Wang, H. Shen, Z. Li, J. Geng, H. Han, J. Cai, X. Li, W. Kang, D. Weng, Y. Lu, D. Wu, L. He, and K. Yao.** 2003. The clinical pathology of severe acute syndrome (SARS): a report from China. J. Pathol. **200:**282–289.
12. **Flaming, K. P., B. L. Goff, D. E. Frank, and J. A. Roth.** 1994. Pigs are relatively resistant to dexamethasone induced immunosuppression. Comp. Hematol. Int. **4:**218–225.
13. **Franks, T. J., P. Y. Chong, P. Chui, J. R. Galvin, R. M. Lourens, A. H. Reid, E. Selbs, C. P. McEvoy, C. D. Hayden, J. Furkuoka, J. K. Taubenberger, and W. D. Travis.** 2003. Lung pathology of severe acute respiratory syndrome (SARS): a study of 8 autopsy cases from Singapore. Hum. Pathol. **34:**743–748.
14. **Fujii, T., T. Nakamura, and A. Iwamoto.** 2004. Current concepts in SARS treatment. J. Infect. Chemother. **10:**1–7.
15. **Gomersall, C. D., M. J. Kargel, and S. E. Lapinsky.** 2004. Pro/con clinical debate: steroids are a key component in the treatment of SARS. Crit. Care **8:**105–107.
16. **Guan, Y., B. J. Zheng, Y. Q. He, X. L. Liu, Z. X. Zhuang, C. L. Cheung, S. W. Luo, P. H. Li, L. J. Zhang, Y. J. Guan, K. M. Butt, K. L. Wong, K. W. Chan, W. Lim, K. F. Shortridge, K. Y. Yuen, J. S. M. Peiris, and L. L. M. Poon.** 2003. Isolation and characterization of viruses related to the SARS coronavirus from animals in Southern China. Science **302:**276–278.
17. **Halbur, P. G., P. S. Paul, E. M. Vaughn, and J. J. Andrews.** 1993. Experimental reproduction of pneumonia in gnotobiotic pigs with porcine respiratory coronavirus isolate AR310. J. Vet. Diagn. Investig. **5:**184–188.
18. **Herridge, M. S., A. M. Cheung, C. M. Tansey, A. Matte-Martyn, N. Diaz-Granados, F. Al-Saidi, A. B. Cooper, C. B. Guest, C. D. Mazer, S. Mehta, T. E. Stewart, A. Barr, D. Cook, A. S. Slutsky, and the Canadian Critical Care Trials Group.** 2003. One-year outcomes in survivors of the acute respiratory distress syndrome. N. Engl. J. Med. **348:**683–693.
19. **Hill, H. T., J. D. Biwer, R. D. Wood, and R. D. Wesley.** 1989. Porcine respiratory coronavirus isolated from two U.S. swine herds, p. 333–335. *In* T. A. Neuzil (ed.), Proceedings of the American Association of Swine Practitioners. American Association of Swine Practitioners, Des Moines, IA.
20. **Ho, J. C., G. C. Ooi, T. Y. Mok, J. W. Chan, I. Hung, B. Lam, P. C. Wong, P. C. Li, P. L. Ho, W. K. Lam, C. K. Ng. M. S. Ip, K. N. Lai, M. Chan-Yeung, and K. W. Tsang.** 2003. High-dose pulse versus nonpulse corticosteroid regimens in severe acute respiratory syndrome. Am. J. Resp. Crit. Care Med. **168:**1449–1456.
21. **Hong, N., and X. K. Du.** 2004. Avascular necrosis of bone in severe acute respiratory syndrome. Clin. Radiol. **59:**602–608.
22. **Hwang, D. M., D. W. Chamberlain, S. M. Poutanen, D. E. Low, S. L. Asa, and J. Butany.** 2005. Pulmonary pathology of severe acute respiratory syndrome in Toronto. Mod. Pathol. **18:**1–10.
23. **Jabrane, A., C. Girard, and Y. Elazhary.** 1994. Pathogenicity of porcine respiratory coronavirus isolated in Quebec. Can. Vet. J. **35:**86–92.
24. **Kim, L., K. O. Chang, K. Sestak, A. Parwani, and L. J. Saif.** 2000. Development of a reverse transcription-nested polymerase chain reaction assay for differential diagnosis of transmissible gastroenteritis virus and porcine respiratory coronavirus from feces and nasal swabs of infected pigs. J. Vet. Diagn. Investig. **12:**385–388.
25. **Ksiazek, T. G., D. Erdman, C. S. Goldsmith, S. R. Zaki, T. Peret, S. Emery, S. Tong, C. Urbani, J. A. Comer, W. Lim, P. E. Rollin, S. F. Dowell, A. E. Ling, C. D. Humphrey, W. J. Shieh, J. Guarner, C. D. Paddock, P. Rota, B. Fields, J. DeRisi, J. Y. Yang, N. Cox, J. M. Hughes, J. W. LeDuc, W. J. Bellini, L. J. Anderson, and the SARS Working Group.** 2003. A novel coronavirus associated with severe acute respiratory syndrome. N. Engl. J. Med. **348:**1953–1966.
26. **Labarque, G. G., H. J. Nauwynck, K. Van Reeth, and M. B. Pensaert.** 2000. Effect of cellular changes and onset of humoral immunity on the replication of porcine reproductive and respiratory syndrome virus in the lungs of pigs. J. Gen. Virol. **81:**1327–1334.
27. **Lai, S. T.** 2005. Treatment of severe acute respiratory syndrome. Eur. J. Clin. Microbiol. Infect. Dis. **24:**583–591.
28. **Landolt, G. A., A. I. Karasin, L. Phillips, and C. W. Olsen.** 2003. Comparison of the pathogenesis of two genetically different H3N2 influenza A viruses in pigs. J. Clin. Microbiol. **41:**1936–1941.
29. **Lapinsky, S. E., and L. Hawryluck.** 2003. ICU management of severe acute respiratory syndrome. Intensive Care Med. **29:**870–875.
30. **Lau, S. K., P. C. Woo, K. S. Li, Y. Huang, H. W. Tsoi, B. H. Wong, S. S. Wong, S. Y. Leung, K. H. Chan, and K. Y. Yuen.** 2005. Severe acute respiratory syndrome coronavirus-like virus in Chinese horseshoe bats. Proc. Natl. Acad. Sci. USA **102:**14040–14045.
31. **Lee, N., K. C. Allen Chan, D. S. Hui, E. K. Ng, A. Wu, R. W. Chiu, V. W. Wong, P. K. Chan, K. T. Wong, E. Wong, C. S. Cockram, J. S. Tam, J. J. Sung, and Y. M. Lo.** 2004. Effects of early corticosteroid treatment on plasma SARS-associated coronavirus RNA concentrations in adult patients. J. Clin. Virol. **31:**304–309.
32. **Li, W., Z. Shi, M. Yu, W. Ren, C. Smith, J. H. Epstein, H. Wang, G. Crameri, Z. Hu, H. Zhang, J. Zhang, J. McEachern, H. Field, P. Daszak, B. T. Eaton, S. Zhang, and L. F. Wang.** 2005. Bats are natural reservoirs of SARS-like coronaviruses. Science **310:**676–679.
33. **Mer, M., and G. A. Richards.** 1998. Corticosteroids in life-threatening varicella pneumonia. Chest **114:**426–431.
34. **Ng, W. F., K. F. To, W. W. Lam, T. K. Ng, and K. C. Lee.** 2006. The comparative pathology of severe acute respiratory syndrome and avian influenza A subtype H5N1-a review. Hum. Pathol. **37:**381–390.
35. **Nicholls, J. M., L. L. Poon, K. C. Lee, W. F. Ng, S. T. Lai, C. Y. Leung, C. M. Chu, P. K. Hui, K. L. Mak, W. Lim, K. W. Yan, K. H. Chan, N. C. Tsang, Y. Guan, K. Y. Yuen, and J. S. Peiris.** 2003. Lung pathology of fatal severe acute respiratory syndrome. Lancet **361:**1773–1778.
36. **Oba, Y.** 2003. The use of corticosteroids in SARS. N. Engl. J. Med. **348:** 2034–2035.
37. **O'Toole, D., I. Brown, A. Bridges, and S. F. Cartwright.** 1989. Pathogenicity of experimental infection with 'pneumotropic' porcine coronavirus. Res. Vet. Sci. **47:**23–29.
38. **Ottolini, M. G., S. J. Curtis, D. D. Porter, A. Mathews, J. Y. Richardson, V. G. Hemming, and G. A. Prince.** 2002. Comparison of corticosteroids for treatment of respiratory syncytial virus bronchiolitis and pneumonia in cotton rats. Antimicrob. Agents Chemother. **46:**2299–2302.
39. **Poon, L. L., Y. Guan, J. M. Nicholls, K. Y. Yuen, and J. S. Peiris.** 2004. The aetiology, origins, and diagnosis of severe acute respiratory syndrome. Lancet Infect. Dis. **4:**663–671.
40. **Roberts, A., D. Deming, C. D. Paddock, A. Cheng, B. Yount, L. Vogel, B. D. Herman, T. Sheahan, M. Heise, G. L. Genrich, S. R. Zaki, R. Baric, and K. Subbarao.** 2007. A mouse-adapted SARS-coronavirus causes disease and mortality in BALB/c mice. PLos Pathog. **3:**e5.
41. **Rota, P. A., M. S. Oberste, S. S. Monroe, W. A. Nix, R. Campagnoli, J. P. Icenogle, S. Penaranda, B. Bankamp, K. Maher, M. H. Chen, S. Tong, A. Tamin, L. Lowe, M. Frace, J. L. DeRisi, Q. Chen, D. Wang, D. D. Erdman, T. C. Peret, C. Burns, T. G. Ksiazek, P. E. Rollin, A. Sanchez, S. Liffick, B. Holloway, J. Limor, K. McCaustland, M. Olsen-Rasmussen, R. Fouchier, S. Gunther, A. D. Osterhaus, C. Drosten, M. A. Pallansch, L. J. Anderson, and W. J. Bellini.** 2003. Characterization of a novel coronavirus associated with severe acute respiratory syndrome. Science **300:**1394–1399.
42. **Saif, L. J.** 2004. Animal coronaviruses: what can they teach us about the severe acute respiratory syndrome? Rev. Sci. Tech. **23:**643–660.
43. **Saif, L. J., L. A. Ward, L. Yuan, B. I. Rosen, and T. L. To.** 1996. The gnotobiotic piglet as a model for studies of disease pathogenesis and immunity to human rotaviruses. Arch. Virol. **12**(Suppl.)**:**153–161.
44. **Saif, L. J., and R. D. Wesley.** 1999. Transmissible gastroenteritis and porcine respiratory coronavirus, p. 295–326. *In* B. Straw (ed.), Diseases of swine, 8th ed. Iowa State University Press, Ames.
45. **Shimizu, M., and Y. Shimizu.** 1979. Effects of ambient temperatures on clinical and immune responses of pigs infected with transmissible gastroenteritis virus. Vet. Microbiol. **4:**109–116.

46. **Simkins, R. A., P. A. Weilnau, J. Bias, and L. J. Saif.** 1992. Antigenic variation among transmissible gastroenteritis virus (TGEV) and porcine respiratory coronavirus strains detected with monoclonal antibodies to the S protein of TGEV. Am. J. Vet. Res. **53:**1253–1258.
47. **Simkins, R. A., P. A. Weilnau, J. Van Cott, T. A. Brim, and L. J. Saif.** 1993. Competition ELISA, using monoclonal antibodies to the transmissible gastroenteritis virus (TGEV) S protein, for serologic differentiation of pigs infected with TGEV or porcine respiratory coronavirus. Am. J. Vet. Res. **54:**254–259.
48. **Snijder, E. J., P. J. Bredenbeek, J. C. Dobbe, V. Thiel, J. Ziebuhr, L. L. Poon, Y. Guan, M. Rozanov, W. J. Spaan, and A. E. Gorbalenya.** 2003. Unique and conserved features of genome and proteome of SARS-coronavirus, early split-off from the coronavirus group 2 lineage. J. Mol. Biol. **331:**991–1004.
49. **So, L. K., A. C. Lau, L. Y. Yam, T. M. Cheung, E. Poon, R. W. Yung, and K. Y. Yuen.** 2003. Development of a standard treatment protocol for severe acute respiratory syndrome. Lancet **361:**1615–1617.
50. **Tingstedt, J. E., D. Tornehave, P. Lind, and J. Nielsen.** 2003. Immunohistochemical detection of SWC3, CD2, CD3, CD4, and CD8 antigens in paraformaldehyde fixed and paraffin embedded porcine lymphoid tissue. Vet. Immunol. Immunopathol. **94:**123–132.
51. **Tse, G. M., K. F. To, P. K. Chan, A. W. Lo, K. C. Ng, A. Wu, N. Lee, H. C. Wong, S. M. Mak, K. F. Chan, D. S. Hui, J. J. Sung, and H. K. Ng.** 2004. Pulmonary pathological features in coronavirus associated severe acute respiratory syndrome (SARS). J. Clin. Pathol. **57:**260–265.
52. **Tsunemitsu, H., D. R. Smith, and L. J. Saif.** 1999. Experimental inoculation of adult dairy cows with bovine coronavirus and detection of coronavirus in feces by RT-PCR. Arch. Virol. **144:**167–175.
53. **VanCott, J. L., T. A. Brim, R. A. Simkins, and L. J. Saif.** 1993. Isotype-specific antibody-secreting cells to transmissible gastroenteritis virus and porcine respiratory coronavirus in gut- and bronchus-associated lymphoid tissues of suckling pigs. J. Immunol. **150:**3990–4000.
54. **van der Hoek, L., K. Pyrc, M. F. Jebbink, W. Vermeulen-Oost, R. J. Berkhout, K. C. Wolthers, P. M. Wertheim-van Dillen, J. Kaandrop, J. Spaargaren, and B. Berkhout.** 2004. Identification of a new human coronavirus. Nat. Med. **10:**368–373.
55. **Van Reeth, K., G. Labarque, H. Hauwynck, and M. Pensaert.** 1999. Differential production of proinflammatory cytokines in the pig lung during different respiratory virus infections: correlations with pathogenicity. Res. Vet. Sci. **67:**47–52.
56. **Wang, H., Y. Ding, X. Li, L. Yang, W. Zhang, and W. Kang.** 2003. Fetal aspergillosis in a patient with SARS who was treated with corticosteroids. N. Engl. J. Med. **349:**507–508.
57. **Wong, S. S., and K. Y. Yuen.** 2005. The severe acute respiratory syndrome (SARS). J. Neurovirol. **11:**455–468.
58. **Yang, M., M. H. Ng, and C. K. Li.** 2005. Thrombocytopenia in patients with severe acute respiratory syndrome (review). Hematology **10:**101–105.
59. **Yang, Z. Y., H. C. Werner, W. P. Kong, K. Leung, E. Traggiai, A. Lanzavecchia, and G. J. Nabel.** 2005. Evasion of antibody neutralization in emerging severe acute respiratory syndrome coronaviruses. Proc. Natl. Acad. Sci. USA **102:**797–801.
60. **Yount, B., R. S. Roberts, A. C. Sims, D. Deming, M. B. Frieman, J. Sparks, M. R. Denison, N. Davis, and R. S. Baric.** 2005. Severe acute respiratory syndrome coronavirus group-specific open reading frames encode nonessential functions for replication in cell cultures and mice. J. Virol. **79:**14909–14922.
61. **Zhong, N. S., and G. W. Wong.** 2004. Epidemiology of severe acute respiratory syndrome (SARS): adults and children. Paediatr. Respir. Rev. **5:**270–274.